J. Nonlinear Funct. Anal. 2021 (2021), Article ID 20 https://doi.org/10.23952/jnfa.2021.20

MATHRES Journal of Nonlinear Functional Analysis
Available online at http://jnfa.mathres.org

ERROR ANALYSIS OF INTERPOLATED COEFFICIENT FINITE ELEMENTS FOR NONLINEAR FRACTIONAL PARABOLIC EQUATIONS

YUELONG TANG*, YUCHUN HUA

College of Science, Hunan University of Science and Engineering, Yongzhou, China

Abstract. In this paper, we consider a fully discrete approximation scheme for nonlinear fractional parabolic equations. The main aim of this paper is to investigate the convergence and superconvergence of interpolated coefficient finite element solutions. Some numerical examples are presented to demonstrate our theoretical results.

Keywords. Nonlinear fractional parabolic equations; Interpolated coefficient finite element approximation; Convergence analysis; Superconvergence analysis.

1. INTRODUCTION

Due to the remarkable memory and hereditary properties, fractional partial differential equations (FPDEs) are more suitable to describe memory and hereditary systems than integer-order partial differential equations (PDEs). They play a very important role in wave propagation, finance, physics, engineering and so on (see, e.g., [1, 2] and the references therein). Since the exact solutions of most FPDEs are very difficult to obtain, many numerical methods were presented, such as, finite difference methods [3, 4, 5], finite element methods (FEMs) [6, 7, 8, 9, 10], mixed FEMs [11, 12], space-time FEMs [13], finite volume methods [14], spectral methods [15, 16, 17] and so on.

FEMs were widely investigated for solving different types of PDEs. For some results on the superconvergence of FEMs for PDEs, we refer the reader to [18, 19, 20, 21]. Generally speaking, there are three kinds of superconvergence. The first one is in certain sampling points, the values in derivatives of errors between the finite element solution and the exact solution with a higher order of convergence than elsewhere [22]. The second one is the gradient in the L^2-norm of errors between the finite element solution and the projection of the exact solution with a greater accuracy than the optimal order of convergence. The third one can be obtained via the post-processing technique. That is, we can reconstruct a greater accuracy gradient according to

*Correspoinding author.
E-mail addresses: tangyuelonga@163.com (Y. Tang), 86592314@qq.com (Y. Hua).
Received February 8, 2021; Accepted May 18, 2021.

©2021 Journal of Nonlinear Functional Analysis

finite element solution. The representative post-processing techniques were developed based on interpolation [23, 24], extrapolation [25] and gradient recovery, which includes superconvergent patch recovery (SPR) [26], polynomial preserving recovery (PPR) [27, 28] and supercovergent cluster recovery (SCR) [29].

For nonlinear parabolic PDEs, an interpolated coefficient finite element method (ICFEM) was originally introduced in [30] and [31]. Its key feature is not to directly discrete the unknown function of the nonlinear term in origin equation but to utilize the interpolation of the nonlinear term under the nodal basis. Then the computational cost of the Jacobi matrix can be greatly reduced when the nonlinear system of the origin equation is solved by the Newton-like method. Recently, this technique has been extended to semilinear elliptic problems [32, 33] or elliptic optimal control problems [34].

In recent years, the superconvergence of FEMs and mixed FEMs for FPDEs were investigated in [35] and [36], respectively. In [37], the superconvergence of nonconforming FEMs for FPDEs was obtained. The above supercovergence results are just suitable for rectangular meshes. However, there few results available on FEMs for semilinear or nonlinear FPDEs. The main purpose of this paper is to investigate a fully discrete ICFEM approximation based on triangular meshes for semilinear time FPDEs and establish the convergence and superconvergence results.

We are concerned with the following semilinear time fractional parabolic equation:

$$\begin{cases} \partial_t^\alpha y(t,x) - \operatorname{div}(A(x)\nabla y(t,x)) + \phi(y(t,x)) = f(t,x), & t \in J, x \in \Omega, \\ y(t,x) = 0, & t \in J, x \in \partial\Omega, \\ y(0,x) = y_0(x), & x \in \Omega, \end{cases} \tag{1.1}$$

where $\partial_t^\alpha\,(0<\alpha<1)$ denotes the α-order left Caputo derivative with respect to the variable t, defined by

$$\partial_t^\alpha y(t,x) = \frac{1}{\Gamma(1-\alpha)} \int_0^t \frac{1}{(t-s)^\alpha} \frac{\partial y(s,x)}{\partial s} ds,$$

$J=[0,T]\,(0<T<+\infty)$, Ω is a bounded open domain of $R^d\,(1\le d\le 3)$ with smooth boundary $\partial\Omega$, $A(x)=(a_{ij}(x))_{d\times d}\in (W^{1,\infty}(\bar{\Omega}))^{d\times d}$ is a symmetric positive definite matrix, the nonlinear function $\phi(\cdot)\in W^{1,\infty}(-R,R)$ for any $R>0$, $\phi'(\cdot)\in L^2(\Omega)$, $\phi'(\cdot)\ge 0$, $f(t,x)$, and $y_0(x)$ are given smooth functions.

Throughout the paper, $L^s(J;W^{m,q}(\Omega))$ denotes all L^s integrable functions from J into $W^{m,q}(\Omega)$ with norm $\|v\|_{L^s(J;W^{m,q}(\Omega))} = \left(\int_0^T \|v\|^s_{W^{m,q}(\Omega)} dt\right)^{\frac{1}{s}}$ for $s\in[1,\infty)$ and the standard modification for $s=\infty$, where $W^{m,q}(\Omega)$ is standard Sobolev spaces on Ω. Similarly, one can define $H^l(J;W^{m,q}(\Omega))$ and $C^k(J;W^{m,q}(\Omega))$ (see, e.g., [38]). In addition, c or C is a generic positive constant.

The rest of this paper is organized as follows. In Section 2, we give a fully discrete ICFEM approximation of (1.1). Convergence analysis results are presented in Section 3. In Section 4, we derive the superconvergence between the numerical solution and the elliptic projection of the exact solution. In Section 5, some numerical examples are presented to support our theoretical results.

2. Interpolated Coefficient Finite Elements Approximation

In this section, we construct a kind of fully discrete ICFEM approximation scheme of (1.1). First, we introduce finite element spaces for the spatial discretization. Next, we denote $W^{m,2}(\Omega)$ by $H^m(\Omega)$ and drop Ω or J whenever possible, i.e.,

$$\|\cdot\|_{m,2,\Omega} = \|\cdot\|_{m,2} = \|\cdot\|_m, \quad \|\cdot\|_0 = \|\cdot\|,$$
$$\|\cdot\|_{L^p(J;W^{m,2}(\Omega))} = \|\cdot\|_{L^p(H^m)}, \quad \|\cdot\|_{L^p(J;W^{m,q}(\Omega))} = \|\cdot\|_{L^p(W^{m,q})}.$$

Furthermore, we set $H_0^1(\Omega) \equiv \{v \in H^1(\Omega) : v|_{\partial\Omega} = 0\}$, and $W = H_0^1(\Omega)$, $U = L^2(\Omega)$. In addition,

$$a(v,w) = \int_\Omega (A\nabla v)\cdot\nabla w, \qquad \forall\, v, w \in W,$$
$$(f_1, f_2) = \int_\Omega f_1 \cdot f_2, \qquad \forall\, f_1, f_2 \in U.$$

Note that A is a symmetric positive matrix. Hence,

$$a(v,v) \geq c\|v\|_1^2, \quad |a(v,w)| \leq C\|v\|_1\|w\|_1, \qquad \forall\, v, w \in W.$$

By using the variational principle, we recast (1.1) as the following weak formulation:

$$\begin{cases} (\partial_t^\alpha y, w) + a(y,w) + (\phi(y), w) = (f, w), & w \in W, t \in J, \\ y(0,x) = y_0(x), & x \in \Omega. \end{cases} \tag{2.1}$$

Let $\mathscr{T}^h$ be a family of quasi-uniform triangulations of Ω such that $\bar{\Omega} = \bigcup_{K\in\mathscr{T}^h} \bar{K}$, and $h = \max_{K\in\mathscr{T}^h}\{h_K\}$, where h_K is the diameter of the element K. Furthermore, we set

$$V_h = \text{span}\{\varphi_i(x) \in C(\bar{\Omega}) : \varphi_i(x) \in \mathbb{P}_1, i = 1, 2, \cdots, M\},$$

where $\{\varphi_i(x)\}_{i=1}^M$ is the nodal basis function with respect to the nodal set $\{x_i\}_{i=1}^M$, and $\mathbb{P}_1$ represents the space of all polynomials whose degree at most 1, and $W_h = V_h \cap H_0^1(\Omega)$.

Then the semi-discrete finite element approximation of (2.1) reads as

$$\begin{cases} (\partial_t^\alpha y_h, w_h) + a(y_h, w_h) + (\phi(y_h), w_h) = (f, w_h), & \forall\, w_h \in W_h, t \in J, \\ y_h^0(x) = y_0^h(x), \end{cases} \tag{2.2}$$

where $y_0^h(x) \in W_h$ is a suitable projection of $y_0(x)$.

Second, we will investigate the $L1$ approximation for the temporal discretization.

Let $0 = t_0 < t_1 < \cdots < t_N = T$ be a given uniform partition of $[0,T]$ with time step $\tau = \frac{T}{N}$, and $t_n = n\tau, n = 0, 1, \cdots, N$. We set $\sigma^n = \sigma(t_n, x)$, and $\partial_t y^n = \frac{y^n - y^{n-1}}{\tau}$. The time fractional derivative can be approximated as follows

$$\partial_t^\alpha y^n = \frac{1}{\tau^\alpha \Gamma(2-\alpha)} \sum_{k=0}^n b_k^n y^k + r_\tau^n := L_t^\alpha y^n + r_\tau^n, \tag{2.3}$$

where $b_k = (k+1)^{1-\alpha} - k^{1-\alpha}$, $b_0^n = (n-1)^{1-\alpha} - n^{1-\alpha}$, $b_n^n = 1$, $b_k^n = b_{n-k} - b_{n-k-1}$ and r_τ^n is the truncation error. It follows from [24] that if $y \in W^{2,\infty}(L^2)$, then

$$\left|r_\tau^n\right| = \left|\partial_t^\alpha y^n - L_t^\alpha y^n\right| \leq C\tau^{2-\alpha}. \tag{2.4}$$

Then the classical fully discrete finite element approximation scheme of (2.1) writes as

$$\begin{cases} (L_t^\alpha y_h^n, w_h) + a(y_h^n, w_h) + (\phi(y_h^n), w_h) = (f^n, w_h), & \forall w_h \in W_h, n = 1, 2, \cdots, N, \\ y_h^0 = y_0^h(x). \end{cases} \tag{2.5}$$

To solve this nonlinear system by Newton-like method, one has to calculate its Jacobi matrix, which depends on the choice of y_h^n, and needs to repeatedly compute. The computation cost is vast. By introducing an interpolation operator $I_h : C(\bar{\Omega}) \to V_h$, for any $w \in C(\bar{\Omega})$, defined by

$$I_h w = \sum_{j=1}^{M} w(x_j)\varphi_j(x)$$

and replacing $\phi(y_h^n)$ with $I_h\phi(y_h^n)$ in (2.5), we have that the Jacobi matrix can be easily calculated.

A fully discrete ICFEM approximation scheme of (2.1) is as follows

$$\begin{cases} (L_t^\alpha y_h^n, w_h) + a(y_h^n, w_h) + (I_h\phi(y_h^n), w_h) = (f^n, w_h), & \forall w_h \in W_h, n = 1, 2, \cdots, N, \\ y_h^0 = y_0^h(x). \end{cases} \tag{2.6}$$

Usually, we set $y_0^h(x) = P_h y_0(x)$, where P_h is an elliptic projection operator (it will be specified later).

From the theory of finite elements [31], for $0 \le m \le r$ and $1 \le p \le \infty$, we have the following error estimate

$$\|I_h w - w\|_{m,p,K} \le Ch^{r-m}\|w\|_{r,p,K}, \qquad \forall w \in C(\bar{\Omega}) \cap W^{r,p}(K), \forall K \in \mathscr{T}^h. \tag{2.7}$$

3. Convergence Analysis

We will derive the convergence of the numerical solution in (2.6). Let P_h be the elliptic projection operator, for any $v \in W$, defined by

$$a(v - P_h v, w_h) = 0, \qquad \forall w_h \in W_h.$$

It has the following error estimates (see [8]):

$$\|v - P_h v\| + h\|\nabla(v - P_h v)\| \le Ch^2\|v\|_2. \tag{3.1}$$

The following conclusions will be used in the following error analysis.

Lemma 3.1. [12] *Let $\{\xi^n\}_{n=0}^N$ be a sequence of functions on Ω. Then*

$$\left(\xi^n, \sum_{k=0}^{n} b_k^n \xi^k\right) = \frac{1}{2}\left(\|\xi^n\|^2 + \sum_{k=0}^{n-1} b_k^n \|\xi^k\|^2 - \sum_{k=0}^{n-1} b_k^n \|\xi^k - \xi^n\|^2\right).$$

Lemma 3.2. [36] *Let $\varphi^k \ge 0$ $(k = 1, 2, \cdots)$, $\varphi^0 = 0$, $\gamma > 0$, and $\varphi^n \le -\sum_{k=1}^{n-1} b_k^n \varphi^k + \gamma$. Then*

$$\varphi^n \le C\tau^{-\alpha}\gamma.$$

Theorem 3.3. *Let y and y_h be the solutions of (2.1) and (2.6), respectively. Suppose that $y \in W^{2,\infty}(L^2) \cap W^{1,\infty}(H^2)$. Then, for any integer $1 \le n \le N$,*

$$\|y^n - y_h^n\| \le C\left(h^2 + \tau^{2-\alpha}\right), \tag{3.2}$$

$$\|y^n - y_h^n\|_1 \le C\left(h + \tau^{2-\alpha}\right). \tag{3.3}$$

Proof. From (2.3) and the definition of P_h, we can rewrite (2.1) at t_n as

$$(L_t^\alpha y^n, w_h) + a(P_h y^n, w_h) + (\phi(y^n), w_h) + (r_\tau^n, w_h) = (f^n, w_h), \qquad \forall w_h \in W_h. \tag{3.4}$$

Setting $\theta^n = y_h^n - P_h y^n$ and subtracting (3.4) from (2.6), for any $w_h \in W_h$, we get

$$(L_t^\alpha \theta^n, w_h) + a(\theta^n, w_h) + (I_h\phi(y_h^n) - \phi(y^n), w_h) = (r_\tau^n, w_h) + (L_t^\alpha(y^n - P_h y^n), w_h). \tag{3.5}$$

Taking $w_h = \theta^n$ in (3.5), we have

$$\begin{aligned} &(L_t^\alpha \theta^n, \theta^n) + a(\theta^n, \theta^n) + (\phi(y_h^n) - \phi(P_h y^n), \theta^n) \\ &= (\phi(y_h^n) - I_h\phi(y_h^n), \theta^n) + (\phi(y^n) - \phi(P_h y^n), \theta^n) + (r_\tau^n, \theta^n) + (L_t^\alpha(y^n - P_h y^n), \theta^n). \end{aligned} \tag{3.6}$$

Note that $a(\theta^n, \theta^n) \geq 0$ and $\phi'(\cdot) \geq 0$. It follows that

$$(\phi(y_h^n) - \phi(P_h y^n), \theta^n) \geq c\|\theta^n\|^2. \tag{3.7}$$

From Lemma 3.1, we have

$$(L_t^\alpha \theta^n, \theta^n) = \frac{1}{2\tau^\alpha \Gamma(2-\alpha)} \left(\|\theta^n\|^2 + \sum_{k=0}^{n-1} b_k^n \|\theta^k\|^2 - \sum_{k=0}^{n-1} b_k^n \|\theta^k - \theta^n\|^2 \right). \tag{3.8}$$

From (2.4), (2.7), (3.1), Hölder's inequality and Young's inequality with ε, we obtain

$$\begin{aligned} &(\phi(y_h^n) - I_h\phi(y_h^n), \theta^n) + (\phi(y^n) - \phi(P_h y^n), \theta^n) + (r_\tau^n, \theta^n) + (L_t^\alpha(y^n - P_h y^n), \theta^n) \\ &\leq (\|\phi(y_h^n) - I_h\phi(y_h^n)\| + \|\phi(y^n) - \phi(P_h y^n)\| + \|r_\tau^n\| + \|L_t^\alpha(y^n - P_h y^n)\|)\|\theta^n\| \\ &\leq C_\varepsilon \left(\tau^{2(2-\alpha)} + \left(\|\phi(y_h^n)\|_2^2 + \|y^n\|_2^2 + L_t^\alpha \|y^n\|_2^2 \right) h^4 \right) + 4\varepsilon \|\theta^n\|^2 \\ &\leq C_\varepsilon \left(\tau^{2(2-\alpha)} + h^4 \right) + 4\varepsilon \|\theta^n\|^2. \end{aligned} \tag{3.9}$$

From (3.6)-(3.9) and $b_k^n < 0 (0 \leq k < n)$, we see that if ε is small enough, then

$$\|\theta^n\|^2 \leq -\sum_{k=0}^{n-1} b_k^n \|\theta^k\|^2 + 2\tau^\alpha \Gamma(2-\alpha) C_\varepsilon \left(\tau^{2(2-\alpha)} + h^4 \right). \tag{3.10}$$

With the help of Lemma 3.2, we have

$$\|\theta^n\| \leq C\left(\tau^{2-\alpha} + h^2 \right). \tag{3.11}$$

Hence, (3.2) follows from (3.1), and (3.11) immediately. Subtracting (2.6) from (2.1), we obtain

$$(L_t^\alpha(y^n - y_h^n), w_h) + a(y^n - y_h^n, w_h) + (\phi(y^n) - I_h\phi(y_h^n), w_h) + (r_\tau^n, w_h) = 0. \tag{3.12}$$

From the assumption on $A(x)$ and (3.12), we arrive at

$$\begin{aligned} c\|y^n - y_h^n\|_1^2 \leq & a(y^n - y_h^n, y^n - y_h^n) \\ = & a(y^n - y_h^n, y^n - P_h y^n) + a(y^n - y_h^n, P_h y^n - y_h^n) \\ = & a(y^n - y_h^n, y^n - P_h y^n) + (L_t^\alpha(y^n - y_h^n), y_h^n - P_h y^n) \\ & + (\phi(y^n) - I_h\phi(y_h^n), y_h^n - P_h y^n) + (r_\tau^n, y_h^n - P_h y^n). \end{aligned} \tag{3.13}$$

From (2.4), (2.7), (3.1)-(3.2), (3.13), Hölder's inequality and Young's inequality, we get

$$\|y^n - y_h^n\|_1^2 \leq C\|y^n - y_h^n\|_1 \|y^n - P_h y^n\|_1 + C(\tau^{4-2\alpha} + h^4). \tag{3.14}$$

Thus, (3.3) follows from (3.1), (3.14), and Poincaré's inequality immediately. This completes the proof. □

4. Superconvergence Analysis

In this section, we derive the global superconvergence results between the interpolated coefficient finite element solution and the elliptic projection of the exact solution.

Theorem 4.1. *Let y and y_h be the solutions of (2.1) and (2.6), respectively. Assume that all the conditions in Theorem 3.3 are valid. Then, for any integer $1 \le n \le N$,*

$$\|P_h y^n - y_h^n\|_1 \le C(h^2 + \tau^{2-\alpha}). \tag{4.1}$$

Proof. Set $y^n - y_h^n = y^n - P_h y^n + P_h y^n - y_h^n := \eta^n + \zeta^n$. Choosing $v = w_h$ in (2.1) and subtracting (2.6) from (2.1), we obtain the error equation

$$(L_t^\alpha (y^n - y_h^n), w_h) + a(y^n - y_h^n, w_h) + (\phi(y^n) - I_h\phi(y_h^n), w_h) + (r_\tau^n, w_h) = 0. \tag{4.2}$$

By using the definition of P_h and (4.2), we have

$$\begin{aligned}(L_t^\alpha \zeta^n, w_h) + a(\zeta^n, w_h) =& (I_h\phi(y_h^n) - \phi(y_h^n), w_h) + (\phi(y_h^n) - \phi(P_h y^n), w_h) \\ &+ (\phi(P_h y^n) - \phi(y^n), w_h) - (L_t^\alpha \eta^n, w_h) - (r_\tau^n, w_h).\end{aligned} \tag{4.3}$$

From the assumption on $A(x)$ and Lemma 3.1, we get

$$\begin{aligned}c(\nabla\zeta^n, \nabla(L_t^\alpha \zeta^n)) &= \frac{c}{2\tau^\alpha\Gamma(2-\alpha)}\left(\|\nabla\zeta^n\|^2 + \sum_{k=0}^{n-1} b_k^n \|\nabla\zeta^k\|^2 - \sum_{k=0}^{n-1} b_k^n \|\nabla\left(\zeta^k - \zeta^n\right)\|^2\right) \\ &\le a(\zeta^n, L_t^\alpha \zeta^n).\end{aligned} \tag{4.4}$$

It follows from Hölder's inequality and Young's inequality with ε, we obtain

$$(I_h\phi(y_h^n) - \phi(y_h^n), L_t^\alpha \zeta^n) \le C\|I_h\phi(y_h^n) - \phi(y_h^n)\|\|L_t^\alpha \zeta^n\| \le C_\varepsilon h^4 \|\phi(y_h^n)\|_2^2 + \varepsilon\|L_t^\alpha \zeta^n\|^2, \tag{4.5}$$

and

$$(\phi(y_h^n) - \phi(P_h y^n), L_t^\alpha \zeta^n) \le C\|y_h^n - P_h y^n\|\|L_t^\alpha \zeta^n\| \le C_\varepsilon(\tau^{2-\alpha} + h^2)^2 + \varepsilon\|L_t^\alpha \zeta^n\|^2. \tag{4.6}$$

In addition,

$$(\phi(P_h y^n) - \phi(y^n), L_t^\alpha \zeta^n) \le C\|P_h y^n - y^n\|\|L_t^\alpha \zeta^n\| \le C_\varepsilon h^4 \|y^n\|_2^2 + \varepsilon\|L_t^\alpha \zeta^n\|^2. \tag{4.7}$$

From $y \in W^{1,\infty}(H^2)$ and (2.3), we see that there holds

$$\begin{aligned}\|L_t^\alpha \eta^n\| =& \left\| \frac{1}{\tau^{\alpha-1}\Gamma(2-\alpha)} \sum_{k=0}^{n-1} b_k \partial_t \eta^{n-k} \right\| \\ \le& \frac{1}{\tau^{\alpha-1}\Gamma(2-\alpha)} \sum_{k=0}^{n-1} b_k \|\partial_t \eta^{n-k}\| \\ \le& \frac{1}{\tau^\alpha\Gamma(2-\alpha)} \sum_{k=0}^{n-1} b_k \int_{t_{n-k-1}}^{t_{n-k}} \|\eta_t\| dt \\ \le& Ch^2 \|y_t\|_{L^\infty(H^2)}.\end{aligned} \tag{4.8}$$

From Hölder's inequality, Young's inequality with ε and (3.1), we conclude that

$$(L_t^\alpha \eta^n, L_t^\alpha \zeta^n) \le \|L_t^\alpha \eta^n\|\|L_t^\alpha \zeta^n\| \le C_\varepsilon h^4 + \varepsilon\|L_t^\alpha \zeta^n\|^2. \tag{4.9}$$

In the same way, we have

$$(r_\tau^n, L_t^\alpha \zeta^n) \le \|r_\tau^n\| \|L_t^\alpha \zeta^n\| \le C_\varepsilon \tau^{4-2\alpha} + \varepsilon \|L_t^\alpha \zeta^n\|^2. \tag{4.10}$$

Setting $w_h = L_t^\alpha \zeta^n$ in (4.3) and noticing that $b_k^n < 0 (0 \le k < n)$, we obtain from (4.4)-(4.10) that

$$\|\nabla \zeta^n\|^2 \le -\sum_{k=0}^{n-1} b_k^n \|\nabla \zeta^k\|^2 + C\tau^\alpha (h^2 + \tau^{2-\alpha})^2. \tag{4.11}$$

It follows from (4.11), Lemma 3.2, and Poincaré's inequality that

$$\|\zeta^n\|_1 \le C(h^2 + \tau^{2-\alpha}). \tag{4.12}$$

This completes the proof of Theorem 4.1. □

5. Numerical Experiments

In this section, we present two different numerical examples to support our theoretical results. The following examples numerically deal with codes developed based on AFEPack, which is freely available and the details can be found at [39]. Their discretization schemes are described in Section 2. Then all the nonlinear systems are solved by the Newton iteration method. We denote $||\cdot||_{L^\infty(H^1)}$, and $||\cdot||_{L^\infty(L^2)}$ by $||\cdot||_{1,\infty}$, and $||\cdot||_{0,\infty}$, respectively. The convergence order rate is computed by the following formula:

$$\text{Rate} = \frac{\ln(e_{i+1}) - \ln(e_i)}{\ln(h_{i+1}) - \ln(h_i)},$$

where e_i (e_{i+1}) denotes the error when the spatial partition size is h_i (h_{i+1}).

Example 5.1. This is a 1D example. The data are as follows:

$$\begin{aligned}
&\Omega = [0,1], T = 1, A(x) = 1,\\
&y(t,x) = t\sin(2\pi x),\\
&f(t,x) = \frac{t^{1-\alpha}}{\Gamma(2-\alpha)}\sin(2\pi x) + 4\pi^2 y(t,x) + e^{y(t,x)}.
\end{aligned}$$

For different α values, the errors on a sequence of uniformly refined meshes' size h and time step size τ are shown in Table 1, Table 2 and Table 3. It is easy to see

$$||y - y_h||_{0,\infty} = \mathscr{O}\left(h^2 + \tau^{2-\alpha}\right),$$

$$||y - y_h||_{1,\infty} = \mathscr{O}\left(h + \tau^{2-\alpha}\right),$$

and

$$||P_h y - y_h||_{1,\infty} = \mathscr{O}\left(h^2 + \tau^{2-\alpha}\right).$$

In Figure 1, we show the numerical solution y_h with $\alpha = 0.5$ when $h = \frac{1}{20}$ and $\tau = \frac{1}{30}$.

TABLE 1. Numerical results with $\alpha = 0.05$, Example 5.1.

h	τ	$\|\|y-y_h\|\|_{0,\infty}$	Rate	$\|\|y-y_h\|\|_{1,\infty}$	Rate	$\|\|P_hy-y_h\|\|_{1,\infty}$	Rate
$\frac{1}{10}$	$\frac{1}{10}$	5.765736e-4	—	7.84265e-1	—	5.51456e-2	—
$\frac{1}{20}$	$\frac{1}{20}$	1.512181e-4	1.9309	4.01214e-1	0.9670	1.55184e-2	1.8293
$\frac{1}{40}$	$\frac{1}{40}$	3.818410e-5	1.9856	2.01313e-1	0.9949	4.10581e-3	1.9182
$\frac{1}{80}$	$\frac{1}{80}$	9.581400e-6	1.9947	1.00716e-1	0.9991	1.05429e-3	1.9614

TABLE 2. Numerical results with $\alpha = 0.5$, Example 5.1.

h	τ	$\|\|y-y_h\|\|_{0,\infty}$	Rate	$\|\|y-y_h\|\|_{1,\infty}$	Rate	$\|\|P_hy-y_h\|\|_{1,\infty}$	Rate
$\frac{1}{10}$	$\frac{1}{10}$	1.04067e-3	—	7.84278e-1	—	5.27707e-2	—
$\frac{1}{20}$	$\frac{1}{30}$	2.60273e-4	1.9994	4.01216e-1	0.9670	1.49032e-2	1.8241
$\frac{1}{40}$	$\frac{1}{90}$	6.29681e-5	2.0473	2.01314e-1	0.9949	3.95809e-3	1.9127
$\frac{1}{80}$	$\frac{1}{270}$	1.52366e-5	2.0471	1.00716e-1	0.9992	1.01966e-3	1.9567

TABLE 3. Numerical results with $\alpha = 0.95$, Example 5.1.

h	τ	$\|\|y-y_h\|\|_{0,\infty}$	Rate	$\|\|y-y_h\|\|_{1,\infty}$	Rate	$\|\|P_hy-y_h\|\|_{1,\infty}$	Rate
$\frac{1}{10}$	$\frac{1}{10}$	2.45585e-3	—	7.84361e-1	—	4.55288e-2	—
$\frac{1}{20}$	$\frac{1}{40}$	6.21851e-4	1.9816	4.01229e-1	0.9671	1.28636e-2	1.8235
$\frac{1}{40}$	$\frac{1}{160}$	1.51093e-4	2.0411	2.01315e-1	0.9950	3.43284e-3	1.9058
$\frac{1}{80}$	$\frac{1}{640}$	3.64806e-5	2.0502	1.00717e-1	0.9991	8.89580e-4	1.9482

Example 5.2. This is a 2D example. The data are as follows:

$$\Omega = [0,1]\times[0,1], T = 1.0,$$
$$A(x) = \begin{bmatrix} 1 & 0 \\ 0 & 1 \end{bmatrix},$$
$$y(t,x) = t^2\sin(2\pi x_1)\sin(2\pi x_2),$$
$$f(t,x) = \frac{2t^{2-\alpha}}{\Gamma(3-\alpha)}\sin(2\pi x_1)\sin(2\pi x_2) + 8\pi^2 y(t,x) + [y(t,x)]^3.$$

In Table 4, Table 5 and Table 6, the errors $||y-y_h||_{0,\infty}$, $||y-y_h||_{1,\infty}$ and $||P_hy-y_h||_{1,\infty}$ based on different α values and a sequence of uniformly refined meshes' size h and time step size τ are shown. It is easy to see that $||y-y_h||_{0,\infty}$ and $||P_hy-y_h||_{1,\infty}$ are the second order convergent while $||y-y_h||_{1,\infty}$ is the first order convergent for the mesh size h.

We plot the profile of the numerical solution y_h with $\alpha = 0.5$ at $t = 0.5$ when $h = \frac{1}{40}$ and $\tau = \frac{1}{90}$ in Figure 2.

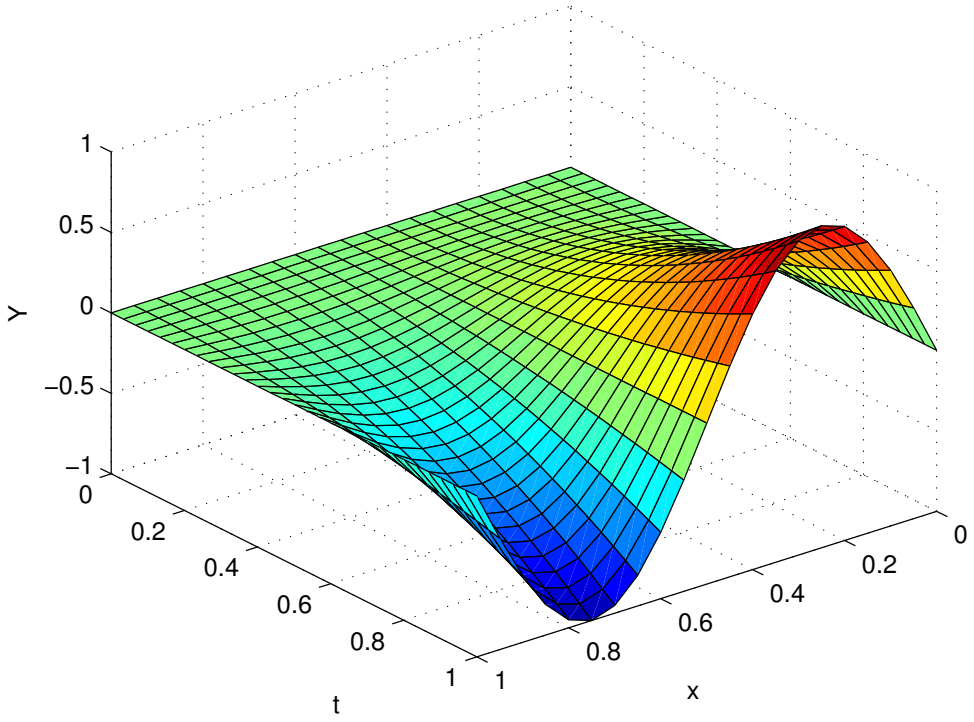

FIGURE 1. The numerical solution y_h with $\alpha = 0.5$, Example 5.1.

TABLE 4. Numerical results with $\alpha = 0.05$, Example 5.2.

h	τ	$\|\|y-y_h\|\|_{0,\infty}$	Rate	$\|\|y-y_h\|\|_{1,\infty}$	Rate	$\|\|P_hy-y_h\|\|_{1,\infty}$	Rate
$\frac{1}{10}$	$\frac{1}{10}$	5.46027e-2	—	1.35784e+0	—	6.76151e-3	—
$\frac{1}{20}$	$\frac{1}{20}$	1.42649e-2	1.9365	6.93043e-1	0.9703	1.71753e-3	1.9770
$\frac{1}{40}$	$\frac{1}{40}$	3.60643e-3	1.9838	3.48334e-1	0.9925	4.31394e-4	1.9933
$\frac{1}{80}$	$\frac{1}{80}$	9.04149e-4	1.9959	1.74395e-1	0.9981	1.08021e-4	1.9977

TABLE 5. Numerical results with $\alpha = 0.5$, Example 5.2.

h	τ	$\|\|y-y_h\|\|_{0,\infty}$	Rate	$\|\|y-y_h\|\|_{1,\infty}$	Rate	$\|\|P_hy-y_h\|\|_{1,\infty}$	Rate
$\frac{1}{10}$	$\frac{1}{10}$	5.42713e-2	—	1.35786e+0	—	9.89283e-3	—
$\frac{1}{20}$	$\frac{1}{30}$	1.41722e-2	1.9371	6.93045e-1	0.9703	2.55023e-3	1.9558
$\frac{1}{40}$	$\frac{1}{90}$	3.58319e-3	1.9837	3.48335e-1	0.9925	6.37628e-4	1.9998
$\frac{1}{80}$	$\frac{1}{270}$	8.98448e-4	1.9957	1.74395e-1	0.9981	1.58427e-4	2.0089

TABLE 6. Numerical results with $\alpha = 0.95$, Example 5.2.

h	τ	$\|\|y - y_h\|\|_{0,\infty}$	Rate	$\|\|y - y_h\|\|_{1,\infty}$	Rate	$\|\|P_h y - y_h\|\|_{1,\infty}$	Rate
$\frac{1}{10}$	$\frac{1}{10}$	5.37094e-2	—	1.35791e+0	—	1.54112e-2	—
$\frac{1}{20}$	$\frac{1}{40}$	1.40080e-2	1.9389	6.93052e-1	0.9704	4.07016e-3	1.9208
$\frac{1}{40}$	$\frac{1}{160}$	3.54122e-3	1.9839	3.48336e-1	0.9925	1.01990e-3	1.9967
$\frac{1}{80}$	$\frac{1}{640}$	8.88084e-4	1.9955	1.74396e-1	0.9981	2.52293e-4	2.0153

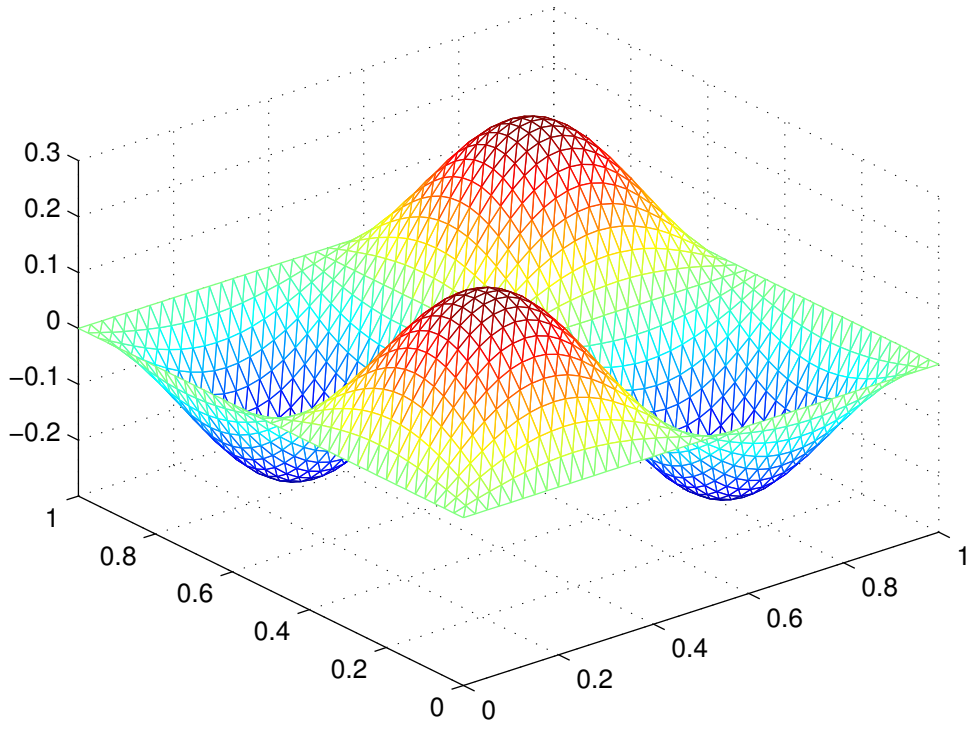

FIGURE 2. The numerical solution y_h with $\alpha = 0.5$ when $t = 0.5$, Example 5.2.

Funding

The first author was supported by the National Natural Science Foundation of China (11401201), the Natural Science Foundation of Hunan Province (2020JJ4323), the Scientific Research Project of Hunan Provincial Department of Education (20A211), and the construct program of applied characteristic discipline in Hunan University of Science and Engineering. The second author was supported by the Scientific Research Project of Hunan Provincial Department of Education (20C0854), and the scientific research program in Hunan University of Science and Engineering (18XKY063, 20XKY059).

REFERENCES

[1] I. Podlubny, Fractional Differential Equations, Academic Press, San Diego, 1999.
[2] F. Zeng, C. Li, F. Liu, I. Turner, Numerical alogrithms for time fractional subdiffusion equation with second-order accuracy, SIAM J. Sci. Comput. 37(1) (2015), A55-A78.
[3] M. Ammi, A. Taakili, Finite difference method for the time-fractional thermistor problem, Int. J. Diff. Equ. 8 (2013), 77-97.
[4] G. Gao, Z. Sun, A compact finite difference scheme for the fractional sub-diffusion equations, J. Comput. Phys. 230 (2011), 586-595.
[5] Y. Lin, C. Xu, Finite difference/spectral approximation for the time-fractional diffusion equation, J. Comput. Phys. 225 (2007), 1533-1552.
[6] L. Chen, R. Nochetto, E. Otárola and A. Salgado, Multilevel methods for nonuniformly elliptic operators and fractional diffusion, Math. Comput. 85 (2016), 2583-2607.
[7] Y. Jiang, J. Ma, High-order finite element methods for time-fractional partial differential equations, J. Comput. Appl. Math. 235 (2011), 3285-3290.
[8] B. Jin, R. Lazarov, J. Pasciak, Z. Zhou, Error analysis of semidiscrete finite element methods for inhomogeneous time-fractional diffusion, IMA J. Numer. Anal. 35 (2015), 561-582.
[9] C. Li, Z. Zhao, Y. Chen, Numerical approximation of nonlinear fractional differential equations with subdiffusion and superdiffusion, Comput. Math. Appl. 62 (2011), 855-875.
[10] R. Nochetto, E. Otárola, A. Salgado, A PDE approach to space-time fractional parabolic problems, SIAM J. Numer, Anal. 54 (2016), 848-873.
[11] Z. Shi, et al., High accuracy analysis of an H^1-Galerkin mixed finite element method for two-dimensional time fractional diffusion equations, Comput. Math. Appl. 74 (2017), 1903-1914.
[12] Y. Zhao, et al., Two mixed finite element methods for time-fractional diffusion equations, J. Sci. Comput. 70 (2017), 407-428.
[13] B. Li, H. Luo, X. Xie, A space-time finite element method for fractional wave problems, Numer. Algor. 85 (2020), 1905-1121.
[14] F. Liu, et al., A new fractional finite volume method for solving the fractional diffusion equation, Appl. Math. Modell. 38 (2014), 3871-3878.
[15] X. Li, C. Xu, A space-time spectral method for the time fractional diffusion equation, SIAM J. Numer. Anal. 47 (2009), 2108-2131.
[16] Z. Mao, J. Shen, Hermite spectral methods for fractional PDEs in unbounded domains, SIAM J. Sci. Comput. 39 (2017), A1928-A1950.
[17] M. Zheng, et al., A high-order spectral method for the multi-term time-fractional diffusion equations, Appl. Math. Model. 40 (2016), 4970-4985.
[18] J. Bramble, A. Schatz, Higher order local accuracy by averaging in the finite element method, Math. Comput. 31 (1997), 74-111.
[19] C. Chen, Y. Huang, High Accuracy Theory of Finite Element Methods, Hunan Science Press, Hunan, China, 1995. (in Chinese).
[20] Q. Lin, Q. Zhu, The Preprocessing and Postprocessing for the Finite Element Method, Shanghai Scientific and Technical Publishers, Shanghai, 1994. (in Chinese).
[21] L. Wahlbin, Superconvergence in Galergin Finite Element Methods, Springer, Berlin, 1995.

[22] J. Barlow, Optimal stress location in finite element method, Internat. J. Numer. Meth. Engrg. 10 (1976), 243-251.
[23] Q. Lin, J. Lin, Finite Element Methods: Accuracy and Improvement, Science Press, Beijing, 2006.
[24] Q. Lin, J. Xu, Linear finite element with high accuracy, J. Comput. Math. 3 (1985), 115-133.
[25] Q. Lin, T. Lu, S. Shen, Maximum norm estimate extrapolation and optimal point of stress for finite element methods on strangly regular triangulation, J. Comput. Math. 1 (1983), 376-383.
[26] O. Zienkiwicz, J. Zhu, The superconvergence patch recovery and a posteriori error estimates, Int. J. Numer. Meth. Eng. 33 (1992), 1331-1382.
[27] A. Naga, Z. Zhang, A posteriori error estimates based on polynomial preserving recovery, SIAM J. Numer, Anal. 42 (2004), 1780-1800.
[28] Z. Zhang, A. Naga, A new finite element gradient recovery method: superconvergence property, SIAM J. Sci. Comput. 26 (2005), 1192-1213.
[29] Y. Huang, N. Yi, The supercovergent cluster recovery method, J. Sci. Comput. 44 (2010), 301-322.
[30] M. Zlámal, A finite element solution for nonlinear parabolic equation, RAIRO Model. Anal. Numer. 14 (1980), 203-216.
[31] S. Larson, V. Tomee, N. Zhang, Interpolation of coefficients and transformation of dependent variable in element methods for the nonlinear heat equation, Math. Meth. Appl. Sci. 11 (1989), 105-124.
[32] Z. Xie, C. Chen, The interpolated coefficient FEM and its application in computing the multiple solutions of semilinear elliptic problems, Int. J. Numer. Anal. Model. 2 (2005), 97-106.
[33] Z. Xiong, Y. Chen, Finite volume element method with interpolated coefficients for two-point boundary value problem of semilinear differential equations, Comput. Meth. Appl. Mech. Eng. 196 (2007), 3798-3804.
[34] Z. Lu, L. Cao, L. Li, Interpolation coefficients mixed finite element methods for general semilinear Dirichlet boundary elliptic optimal control problems, Appl. Anal. 97 (2018), 2496-2509.
[35] C. Huang, M. Stynes, Superconvergence of a finite element method for the multi-term time-fractional diffusion problem, J. Sci. Comput., 82 (2020), 10.
[36] D. Shi, F. Yan, J. Wang, Unconditional superconvergence analysis of a new mixed finite element method for nonlinear Sobolev equation, Appl. Math. Comput. 274 (2016), 182-194.
[37] Y. Zhao, et al., Superconvergence analysis of nonconforming finite element method for two-dimensional time fractional diffusion equations, Appl. Math. Lett. 59 (2016), 38-47.
[38] J. Lions, E. Magenes, Non Homogeneous Boundary Value Problems and Applications, Springer-verlag, Berlin, 1972.
[39] R. Li, W. Liu, The AFEPack Handbook, 2006, https://blog.csdn.net/HateCode/article/details/1413290.